Experimental estimation of the transmission loss contributions of a sound package placed in a double wall structure

Olivier Doutres, Noureddine Atalla

GAUS, Department of mechanical engineering, Université de Sherbrooke (Qc), Canada, J1K 2R1

Email address: olivier.doutres@usherbrooke.ca

Applied Acoustics 72 (2011) 372–379
Preprint version

Authors' accepted manuscript of the article published in
Applied Acoustics, vol. 72 no 6 (May 2011), p. 372-379
https://doi.org/10.1016/j.apacoust.2010.12.011

ABSTRACT

The objective of this paper is to propose a practical impedance tube method to optimize the sound transmission loss of double wall structure by concentrating on the sound package placed inside the structure. In a previous work, the authors derived an expression that breakdown the transmission loss of a double wall structure containing a sound absorbing blanket separated from the panels by air layers in terms of three main contributions; (i) sound transmission loss of the panels, (ii) sound transmission loss of the blanket and (iii) sound absorption due to multiple reflections inside the cavity. The sound transmission loss contributions of the blanket can thus be estimated from three acoustic measurements using impedance tube techniques: two reflection coefficients at the front face and the rear face of the blanket placed in specific positions characteristic of its position inside the double wall structure and its sound transmission coefficient. The method is first validated in the case of a double wall structure filled with a 2 inch foam material. Next, it is applied to investigate (i) the effect of frame compression of a 2 inch fibre glass in an aeronautic-type double wall structure and (ii) the effect of double porosity with or without porous inclusions in a building-type double wall structure.

1. Introduction

The sound transmission performance of double wall systems containing sound absorbing blankets is of utmost importance for noise control in various applications. Measurement of the sound transmission loss of such structures generally requires an important setup consisting of two coupled rooms, e.g. a reverberant and a anechoic one, and large structure to test (usually larger than $1m^2$ to minimise size effects at low frequencies [1]). Testing the influence of various sound packages in the structure is thus expensive and time consuming. The setup could be simplified and the size of the structure to test considerably reduced by measuring its transmission loss in an impedance tube. In that case, the structure must have a one-dimensional behaviour inside the tube which involves a sliding boundary condition. However, such measurement is difficult for highly insulating systems with thin walls. First, the sliding condition is difficult to realize. Usually, the system is bonded along its edges which may induce lateral compression for the sound package [2-5] and undesired resonances for the plates (especially for thin plates as in aircraft applications). Part of the double wall system may also depict air-gaps around its circumference leading to leaks [6]. In addition, the sound transmission loss of the double wall system can be high and use of classical impedance tube methods can show a lack of accuracy due to the very low pressure level downstream the structure.

The objective of this paper is to propose a simple experimental method to estimate the influence of the sound package when placed in a double wall structure. According to the authors' previous work [7], the normal incidence airborne sound transmission loss of a double wall structure, without mechanical links, is written in terms of three main contributions; (i) sound transmission loss of the panels, (ii) sound transmission loss of the blanket and (iii) sound absorption due to multiple reflections inside the cavity. The transmission loss contributions of

the blanket can thus be estimated from three impedance tube measurements: two reflection coefficients of the blanket placed in specific configurations related to its position inside the double wall structure and its sound transmission loss. The above mentioned experimental difficulties involved in transmission loss impedance tube measurements of thin and highly insulating double wall systems are avoided. The method can then be used to quickly investigate the effect of various sound packages or of sound packages which are difficult to model (i.e. complex asymmetric multilayer, compressed blanket, complex interface between materials....) with a view to optimize them.

First, the method and an experimental validation in the case of an aeronautic double wall structure filled in with a 2 inch thick porous foam are presented. Note that detailed numerical validations have been presented in reference [7]. Next, the value of the proposed method is demonstrated by investigating experimentally (i) the effect of compression of fibre glass inside a double wall system with thin walls and (ii) the potential of using the double porosity effect in a building-type double wall structure.

2. Method

A schematic view of the structure is shown in Fig. 1. This structure is a partition consisting of two thin homogeneous panels, separated by an air-gap containing an acoustically absorbing multilayer blanket, and with no mechanical links between the two panels. The air layer between the first panel and the front face of the porous multilayer has a thickness D_1 and is referred to here by the upstream cavity. The air layer between the rear face of the porous layer and the second panel has a thickness D_2 and is referred to by the downstream cavity. The porous multilayer thickness is denoted by d.

The authors recently shown [7] that the use of a wave decomposition of the acoustic field allows one to breakdown the normal incidence sound transmission loss into three main parts as

$$TL = (TL_{p1} + TL_{p2}) + TL_m + (TL_u + TL_d) \quad \text{dB}. \tag{1}$$

TL_{p1} and TL_{p2} account for the sound transmission loss of the first and second panel. For normal incidence, they are simply derived from their surface mass density m_{sj} (j=1,2) as

$$TL_{pj} = -20\log\left(\left|\frac{2Z_0}{2Z_0 + j\omega m_{sj}}\right|\right), \tag{2}$$

with Z_0 the characteristic impedance of the fluid and ω the angular frequency.

TL_m, accounts for the sound transmission loss of the sound absorbing blanket. TL_u and TL_d, account for the multiple wave reflections in the upstream and downstream cavities inside the double wall structure, respectively. They are given by

$$TL_u = -20\log\left(\frac{1}{\left|1 - r_1 r_{p1} e^{-2jk_0 D_1}\right|}\right), \tag{3}$$

and

$$TL_d = -20\log\left(\frac{1}{\left|1 - r_2 r_{p2} e^{-2jk_0 D_2}\right|}\right). \tag{4}$$

These coefficients are derived using the wave decomposition method which takes explicitly into account the multiple wave reflections in the upstream and downstream cavities and makes no assumption on the reflection coefficients. Here, k_0 is the wave number in the fluid. r_1 is the reflection coefficient at the front face of the blanket backed by an air gap of thickness equal to the thickness of the downstream cavity and the second panel. The second panel can be replaced by a rigid and immobile termination in the calculation of r_1, leading to a discrepancy in the estimation of the mechanical behaviour of the double wall structure in the low frequency range around the Double Wall Resonance (DWR) frequency [7]. r_2 is the reflection coefficient at the rear face of the blanket when backed by an infinite air layer. Finally, r_{p1} and r_{p2} are the reflection coefficients of the first and second panels respectively and are also derived knowing the surface mass density of each panel as

$$r_{pj} = \frac{j\omega m_{sj}}{2Z_0 + j\omega m_{sj}}. \tag{5}$$

Contrary to the plates behaviour which can be easily modeled knowing their surface densities (see Eqs. (2) and (5)), the prediction of the multilayer blanket behaviour using the

classical Transfer Matrix Method (TMM) is not straightforward since the non-acoustic properties of each layer constituting the blanket have to be known (i.e. requires independent measurement of their Biot properties) together with the details of the interlayer-interface conditions. The latter are not always known, in real life applications, making modeling of the multilayer with the TMM inaccurate. The alternative proposed in this paper is thus to determine the transmission loss contributions of the sound absorbing blanket (i.e, TL_u, TL_d, TL_m), from three measurements of the blanket acoustic properties (i.e. r_1, r_2 and TL_m) using impedance tube techniques.

It is worth mentioning that because the structure is submitted to normal incidence acoustic excitation, the model used to describe the plates in this paper is valid for frequencies below the critical frequency of the panels. Besides, the blanket transmission loss contributions determined under normal incidence excitation (due to impedance tube measurements) are considered to be sufficiently characteristic of the material behaviour to be used as criteria for real double wall structure optimization. This assumption represents the main practical limitation of the proposed method.

3. Experimental setup

The three different setups to measure the acoustic properties r_1, r_2 and TL_m are depicted in Fig. 2. The reflection coefficients r_1 and r_2 are measured in an impedance tube according to the standard ISO-10534-2 [8]. As shown in figure 2(a), the reflection coefficient r_2 at the rear face of the sample (side **d**) is measured with a semi-infinite air gap at the front face of the sample (side **u**) by the use of an anechoic termination. The reflection coefficients r_1 at the front face is performed with an air gap at the rear face of thickness equal to the thickness of the air layer in the structure (D_2) and followed by the rigid termination of the impedance tube

(see Fig. 2(b)). This last reflection coefficient, called r_1^w in reference [7], will mainly lead to a discrepancy in the estimation of the mechanical behaviour of the double wall structure in the low frequency range around the DWR frequency because it does not account for the mechanical behaviour of the second panel. This discrepancy is not important in this study since the effect of the sound package is mainly investigated in the medium and high frequency ranges, i.e. above the DWR frequency.

Note that, in the case of an asymmetric sound absorbing blanket (i.e. the two faces having different absorbing coefficients), it is of upmost importance to reverse the blanket between the r_1 and r_2 measurements, i.e. perform the r_1 measurement at the font face of the blanket (side **u**) and the r_2 measurement at the rear face (side **d**). This will ensure the correct measurement of the acoustic behaviour of the blanket placed in the double wall structure, i.e. the different absorption behaviours of the blanket in the upstream and downstream cavities.

Fig. 2(c) presents the 3-microphone method recently proposed by Salissou [9] and used here to measure the normal incidence sound transmission loss of the sound absorbing blanket TL_m. This method assumes that only plane waves propagate upstream and downstream the blanket but no assumptions are made on its boundary conditions, shape, and material properties (i.e., the element may be symmetrical or not along its thickness, homogeneous or not, isotropic or not). This method provides identical results compared to general four-microphone methods [9] but the setup is simplified in that it requires only a total of 3 microphones and uses two well-defined air cavities. Note that in the case of a symmetric monolayer blanket, the 4-microphone method proposed by Song and Bolton [10] can be used. Note also that since one of the tests in the presented method requires an anechoic termination, the latter configuration can also be used

to measure the transmission coefficients. The use of the three microphones method in this paper was selected for its simplicity rather than for necessity or better accuracy.

Different impedance tubes have been used for the experimental measurements (see Table 1). Acoustic measurements presented in section 4 and 5.1 were carried out in a 44.5-mm diameter impedance tube and measurements presented in section 5.2 in a 100-mm diameter impedance tube. For each tube configurations, a loudspeaker at one end of the tube generated a broadband random signal in the frequency band given in Table 1. Three BSWA Type MPA416 microphones were used as shown in Fig. 2. Microphones 1 and 2 were at standard positions whereas microphone 3 is flush mounted on the hard termination. Transfer functions between the microphones to compute both r_1, r_2 and TL_m were estimated following the approach described in standard ISO-10534-2 [8]. To minimize the effects of microphone phase mismatch, a microphone switching calibration procedure was used based on ISO-10534-2. The anechoic termination used for the measurement of the reflection coefficient r_2 is constructed using a 4 meter-long cylindrical tube filled with low density fibre glass. The fibre glass is arranged in a way that its density increases gradually as the acoustic wave propagates in the tube. The measured absorption coefficient of the anechoic termination is higher than 98% starting at 150Hz. Note that it is important to measure the ambient conditions of temperature, pressure and humidity rate during measurements to estimate correctly the characteristic impedance Z_0 and wave number in the fluid k_0 required in Eqs. (2)-(5).

4. Validation on a two inch thick foam layer

First, the validity of the proposed experimental method is checked by comparison with a full TMM solution in the case of a double wall configuration made up from a 51mm-thick

melamine foam layer, called material A, centered between two 1mm aluminum panels (m_{s1}= m_{s2}=2.742 kg/m^2). The thicknesses of the upstream and downstream cavities are 25mm (D_1=D_2=25mm).

The TMM solution requires the foam modeling [11]. Since the porous layer is not directly bonded on the vibrating panel in this case, it is considered acoustically limp [11-13], i.e. the frame can move and its inertia effect is taken into account. The foam layer is thus described from its characteristic wave number k and characteristic impedance Z_c. The main six non-acoustic properties required in this equivalent fluid model are bulk density ρ, static airflow resistivity σ, porosity ϕ, tortuosity α_∞, viscous characteristic length Λ, and thermal characteristic length Λ'. Other properties exist but are not investigated in this paper since the main six properties are usually sufficient for engineering analysis in the context of building or transport applications. Here, the density and the porosity are determined from direct measurement [14] and the 4 other using the 3-microphone impedance tube method recently presented elsewhere [15]. Properties of foam A are given in table 2.

Fig. 3 presents TMM simulations and impedance tube measurements of the absorption coefficient related to r_1, r_2 and the sound transmission loss of the foam TL_m. As shown in Fig. 3, there is a good agreement between measurements and simulations except at some local frequencies due to boundary condition impact and frame resonances. In the case of the absorption coefficient related to r_2, the low frequency oscillations appearing in the measurement curve are due to the anechoic termination. Indeed, in the case of a highly absorptive material with low transmission loss such as material A, the low frequency absorption related to r_2 is mainly due to the anechoic termination.

The measured reflection coefficients and sound transmission loss are then used in Eqs. (3) and (4) to determine the sound transmission loss contributions TL_u and TL_d and finally Eq. (1) is used to estimate the normal incidence sound transmission loss of the double wall structure. Fig. 4(a) presents the comparison between the TL of the double wall structure estimated from the proposed method, the TMM simulation and the TL simulation of the empty structure. Note that the simulation of the empty structure is also determined from Eq. (1). In that case, TL_m = 0dB, TL_d =0 dB because r_2=0 and TL_u accounts for both the double wall resonance and the cavity resonances (details are given in ref. [7]). Fig. 4(b) presents the three transmission loss contributions related to the porous layer influence inside the structure: TL_m, TL_u and TL_d. These contributions are determined from measurements or from TMM simulation of r_1, r_2 and TL_m. Fig. 4(b) shows that the proposed experimental determination of the transmission loss contributions of the porous layer TL_u and TL_d from impedance tube measurements gives the same result compared to the TL contributions determined using the reference TMM model. Thus, the proposed experimental determination of double wall structure transmission loss (determined from Eq. (1)) gives the same result compared to the reference TMM model as shown in Fig. 4(a) (see solid black line and circles). The reflection coefficient r_1 being measured in an impedance tube, the second panel is replaced by the rigid termination of the tube. As mentioned in the previous paper [7] and verified in Fig. 4(a), this simplification mainly leads to a discrepancy in the estimation of the mechanical behaviour of the double wall structure in the low frequency range around the DWR frequency (up to 300 Hz in this case).

Note that, as known, the effect of material A starts mainly at the first resonance of the cavity (see Fig. 4(a)); $f=c_0/2(D_1+D_2+d)$~1698 Hz, with c_0 is the speed of sound in air. It attenuates the dips of insulation controlled by the cavity resonances around 1.7 kHz and 3.4 kHz

and improves the insulation at high frequencies. Regarding now the transmission loss contributions, Fig. 4(b) shows that the TL_u and TL_d contributions are inferior to the contribution of the transmission loss of the material TL_m. Whereas the sound transmission loss of the multilayer increases continually with frequency, the sound transmission losses due to upstream and downstream absorptions present slight oscillations around 0dB (the maximum amplitude is inferior to 3dB). Note that these results are not relevant for frequencies below 300Hz because the proposed method, associated with the r_1 measurement including a rigid wall, is not valid under and around the DWR frequency of the structure. In addition, the accuracy of the measurement using the 44.5mm impedance tube and the used anechoic termination are reduced in this frequency range

Since the proposed experimental method has been validated on a simple symmetric porous monolayer, it is now applied to more complicated configurations for which a TMM simulation is more difficult to derive. In the following, the effect of frame compression and double porosity with or without porous inclusions is investigated.

5. Application

5.1 Effect of frame compression on a two inch thick fibre glass material

The first application concerns the effect of the frame compression of a fibre glass material placed in a double wall transmission loss configuration. The configuration studied here consists of two 1 mm thick, aluminum flat panels separated by 101.6 mm (4.0 in.), with a 51 mm (2.0 in) thick layer of fibre glass material placed close to the second panel. Specifically, the downstream cavity D_2 is set to 2 mm and the upstream cavity D_1 to 48.8 mm. The TL of this

configuration is compared to a second configuration in which the fibre glass is compressed in the thickness direction at a compression rate $n=d_0/d_c=2$, where d_0 is the nominal thickness and d_c the compressed thickness. A homemade sample holder shown in Fig. 5 is used to compress the sample. Transmission loss (TL_m) and reflection coefficient (r_1) measurements of a 34.5 mm fibrous layer with and without sample holder have been carried out and it has been checked that the sample holder can be considered acoustically transparent. In the compressed configuration, the downstream cavity D_2 is still set to 2 mm and the upstream cavity D_1 is now set to 74 mm in order to keep the distance between the two panels constant. The fibre glass material, called material B here, is a very light and limp fibrous material usually encountered in aircraft applications. Its properties are given in table 2 and they have been determined using the same method described in section 4 for material A. However, the static airflow resistivity is determined this time using a direct measurement [16]. The airflow resistivity of the 51 mm uncompressed material is σ_0=14 000 N.s.m^{-4} and increases to σ_c=27 700 N.s.m^{-4} for a compression rate n=2. This value is in good agreement with the formula proposed by Castagnède *et al.* in ref [17] and given by $\sigma_c=n\,\sigma_0$.

Fig. 6 presents the absorption coefficient measurements related to r_1 and r_2 and the sound transmission loss TL_m of the fibre glass sample in the uncompressed and compressed configurations. Note that, due to the proposed double wall configuration depicted previously, the downstream cavity D_2 is set to 2 mm in the case of the r_1 measurement. The absorption coefficients presented in Fig. 6(a) corroborate what has been previously observed in refs. [17, 18]: a strong decrease of the absorption coefficient due to the drop in thickness. This absorption decrease is also visible on the absorption behaviour related to r_2, i.e. when the fibrous layer is backed by the anechoic termination. Regarding now the transmission loss of the sample TL_m for

the 2 configurations (see Fig. 6 (c)), it is shown that the compression has little influence on the transmission loss of the sample above 900 Hz. This is plausible since the mass of the sample remain constant during compression and in consequence mass law is conserved. Moreover, the possible TL enhancing effect due to an increase of the airflow resistivity and a decrease of both viscous and thermal lengths associated to the frame compression [17] is compensated by the negative effect of the thickness decrease. Below 900 Hz, each transmission loss shows a minimum at the shearing resonance of the sample [3,4]. Because this mechanical behaviour strongly depends on the sample's edge constraint inside the tube, the results given below this frequency have to be considered with great care (stiffness and size controlled). Note that the frequency of the shearing resonance is higher in the case of the compressed sample because the frame is stiffer.

Fig. 7 presents the sound transmission loss contributions due to the multiple acoustic reflections in the upstream cavity TL_u and downstream cavity TL_d derived from Eqs. (3) and (4) respectively. The variation of the TL_u behaviour between the uncompressed and compressed configuration as shown in Fig. 7(a) is characterized by a frequency shift of the oscillating behaviour. This frequency shift can be attributed to the drop in sample thickness which induces an absorption decrease (see Fig. 6(a)) but also an increase of the upstream cavity thickness D_1. It is shown Fig. 7(a) that the transmission loss contribution TL_u decreases between 1500 Hz and 2500 Hz (with a maximum decrease of 3.5 dB at 1700 Hz) and increases between 500 Hz and 1500 Hz and above 2500 Hz. The transmission loss contribution due to the absorption behaviour in the downstream cavity TL_d is globally decreased because of the sample thickness drop.

The normal incidence sound transmission loss of the double wall structure is finally determined from Eq. (1) for the uncompressed and compressed configurations. Fig. 8(a) presents

these transmission loss curves and a TMM simulation of the sound transmission loss of the empty structure. The effect of the frame compression is investigated more in details in Fig. 8(b) where the Air Borne Insertion Loss (*ABIL*) determined as $ABIL = TL_{\text{compressed}} - TL_{\text{uncompressed}}$ is presented.

Figs. 8(a) and 8(b) show that the frame compression has little effect on the sound transmission loss of the structure at lower frequency (up to 1100 Hz). However, results below 900 Hz should be considered with great care because the TL_m measurements are greatly affected by the sample's edge constraint. Above 1100 Hz, the ABIL shows an oscillating behaviour with a 5dB transmission loss decrease around 1700Hz (close to the first acoustic resonance of the cavity separating the two panels) and a 4 dB increase around 3000 Hz (close to the second acoustic resonance of the cavity separating the two panels). It is worth mentioning that the frequency position of these dips and peaks depends on the position of the material inside the double wall structure (thickness of the cavities D_1 and D_2). Since this behaviour is also due to the absorption behaviour inside the structure (see Eqs.(3) and (4)), the amplitude of these dips and peaks depends on the compression rate applied to the material.

5.2 Effect of double porosity with or without inclusions

The second application concerns the effect of a meso-perforated material with or without porous inclusions placed in a double wall transmission loss configuration generally encountered in the building field. The configuration studied here consisted of two 12.7 mm (0.5 in.) thick, gypsum flat panels separated by 76 mm (3.0 in.), with a 56 mm thick layer of fibrous material centered in that space. The upstream and downstream cavities are 10mm thick (D_1= D_2=10mm). The two panels have a density of 860 kg/m^3 (m_{s1}= m_{s2}=10.92 kg/m^2). The fibrous material is a

standard rockwool which is a very rigid, dense and resistive material. The properties of this material, called material C in this paper, are given in Table 2.

The double porosity configuration consists in a set of periodical perforations in the thickness direction. Several studies, based on analytical, numerical or experimental analysis have shown that the double porosity may enhance considerably the absorption coefficient [11,19,20, 21]. However, Jaouen *et al.* [19] and Gourdon *et al.* [20] pointed out that the absorption properties can be worsened at very low frequency and the transmission loss behaviour considerably affected by the presence of the holes. The effect on the absorption behaviour, of a porous material inclusion in the holes is then investigated analytically and experimentally and it is shown that the inclusion allows improvements especially at low frequencies.

This section uses the proposed method to demonstrate experimentally the effect of a double porosity material with or without porous inclusions on the transmission loss of the double wall structure. More precisely, does the absorption improvement inside the double wall structure induced by the double porosity effect compensate for the transmission loss decrease?

In the proposed configuration, a rockwool is used as frame material (Material C, see Table2) and a melamine foam as inclusions material (Material A, see Table 2) as shown in Fig. 9. Three samples are investigated: the single and double porosity rockwool and the double porosity rockwool with melamine inclusion. For each sample, measurements of r_1, r_2 and TL_m are carried out this time in the large impedance tube (see Table 1). Due to the small impedance tube section, only one periodic cell shown in Fig. 9 is considered, i.e. the external cross section of the sample is circular with only one perforation at its center which is filled or not by a porous inclusion. It is worth noting that this is representative of the periodically perforated material assuming perfect sliding conditions. The diameter of the perforation is set to 44.5mm which

gives a mesoporosity ϕ_p equal to 0.198. According to the criterion proposed by Sgard *et al.* (see Eq.(27) in reference [21]), the high airflow resistivity of the rockwool material coupled to an important value of the mesoporosity ensure a considerable enhancement of the absorption coefficient.

Fig. 10 presents the measured absorption coefficients related to r_1 and r_2 and the sound transmission loss TL_m of the three configurations. According to the geometry of the studied double wall configuration, the downstream cavity D_2 is set to 10 mm in the case of the r_1 measurement. The absorption coefficients presented in Fig. 10 (a) corroborate what has been previously observed by Gourdon *et al.* [20]: (i) compared to single porosity, the double porosity deteriorates the absorption at low frequency (here, up to 350 Hz) but greatly improves the absorption at medium and high frequencies; (ii) compared to double porosity, the double porosity with inclusion improves the absorption behaviour at lower frequency, decreases the amplitude of the peaks and dips to give a better global effect.

Fig. 10 (b) shows that the absorption coefficient of the sample backed by an anechoic termination is enhanced by the presence of the perforation in the whole frequency range and especially at lower frequencies, i.e. up to 400 Hz (see light grey line). This is normal since the dissipated power is the sum of the absorbed power and the transmitted power; the latter being important for the perforated sample. The melamine inclusion in this case decreases the performance of the double porosity in the lower frequency range but still offers better absorption behaviour compared to the fibrous single porosity configuration. Regarding now the sound transmission loss of the sample TL_m for each configuration (see Fig. 10 (c)), it is observed, as expected, that the perforation dramatically decreases the transmission loss of the sample with a relative difference with single porosity configuration close to 15 dB in the whole frequency

range (see black and light grey curves). The addition of the melamine inclusion reduces this difference but still shows a 5dB decrease compared to the single porosity configuration. Note that the three TL_m curves show a mechanical influence of the rockwool frame: (i) the TL_m decrease around 250 Hz is due to a shearing resonance of the sample which is strongly dependant to the boundary conditions [3,4] (ii) multiple TL_m dips around 1000 Hz are due to frame resonances in the thickness of the layer. Thus, the strong influence of the boundary conditions and the use of a rigid termination in the determination of r_1 limit the proposed impedance tube method to recover the sound package behaviour in the double wall structure at very low frequencies. Results in the lower frequency range (up to 300 Hz in this case) should be discarded.

Fig. 11 presents the sound transmission loss contributions due to multiple acoustic reflections in the upstream cavity TL_u and downstream cavity TL_d derived from Eqs. (3) and (4) respectively. It is observed in Fig. 11(a) that the absorption improvement in the upstream cavity due to double porosity results in an increase of the transmission loss contribution TL_u between 200 Hz and 800 Hz; with a maximum increase of 9 dB at 500 Hz. The addition of the melamine inclusion still offers a transmission loss increase compared to single porosity but with a maximum reduced to 4 dB at 400 Hz. The transmission loss contribution TL_d is mainly improved in the case of the double porosity in the low frequency range. It is observed here, that the influence of the blanket absorption inside the double wall structure is mainly visible in the low frequency range, i.e. up to 1000 Hz.

The normal incidence sound transmission loss of the double wall structure is finally determined from Eq. (1) for the three configurations. Fig. 12(a) presents these transmission loss curves and a TMM simulation of the sound transmission loss of the empty double wall. The

effect of the double porosity with or without porous inclusion compared to the single porosity is investigated more in details in Fig. 12(b) where the Airborne Insertion Loss (*ABIL*) determined as $ABIL = TL_{\text{double porosity}} - TL_{\text{single porosity}}$ is presented.

Figs. 12(a) and 12(b) show that the double porosity with or without inclusion has little effect on the sound transmission loss of the structure at low frequency (up to 400 Hz). In this frequency band, the transmission loss decrease observed on TL_m (see Fig. 10(c)) which is due to the perforation is compensated by the absorption enhancement observed on both TL_u and TL_d (see Fig. (11)). However, above this frequency the perforation, filled or not by the melamine foam, does not improve the sound absorption in the cavities and since it deteriorates considerably the sound transmission loss of the sample, it results in an important decrease of the sound insulation of the double wall structure, especially for the non-filled configuration.

6. Conclusion

This paper presented a simple experimental method to estimate the normal incidence sound transmission loss contributions of complex sound packages filling a double wall structure from three impedance tube measurements of the sound package alone. It is based on a new model recently proposed by the authors [7] which allows one to derive the sound transmission loss of the structure from the estimation of the absorption and transmission loss contributions of the sound package inside the structure. The proposed method requires three impedance tube measurements: two reflection coefficients at the front and rear face of the blanket placed in specific positions characteristic of its position inside the double wall structure and its transmission loss coefficient. The method is first validated experimentally in the case of a double wall structure filled with a melamine porous material. Next, it is used to highlight experimentally

the effects of (i) fibrous frame compression and (ii) double porosity with or without porous inclusions on the sound transmission loss of double wall structures. These experimental investigations are shown to corroborate the fact that (i) at high frequencies, the transmission loss contribution of the blanket is preponderant compared to the absorption contributions, (ii) at medium and low frequencies, the absorption performance of the blanket can play an important role. In the case of the double porosity material with or without porous inclusions, the sound transmission loss of the double wall structure at high frequencies is strongly decreased because of the blanket perforations. The good absorption properties of the double porosity material allows to maintain good performance at medium frequencies but do not compensate for the great decrease of sound transmission loss at high frequencies caused by the perforations (filled or not by porous inclusions). In the case of the frame compression of a limp fibre glass, the sound transmission loss of the blanket is barely affected by the compression. However, the absorption behaviour of the compressed blanket inside the double wall structure is greatly affected, i.e. the absorption is decreased due to a thickness effect and the size of the upstream cavity is increased, what modify the transmission loss behaviour of the whole structure.

The proposed method is restricted to frequencies above the double wall resonance of the double wall since the mechanical behaviour of the second panel is not taken into account in the tube measurements and frequencies below the critical frequencies of the panels because only their inertia is taken into account a consequence of the used normal incidence plane wave excitation. Furthermore, it is important that the experimenter ensures that the multilayer blanket behaves as an equivalent fluid (rigid or limp) inside the impedance tube with no contribution of the frame elastic behaviour and with no leakage.

Acknowledgements

The authors would like to thank the National Sciences and Engineering Research Council of Canada (NSERC) for providing financial support and P. Lévesque for its contribution to design of the different setups presented in this work.

References

1. Anonymous, "Standard Test Method for Laboratory Measurement of Airborne Transmission Loss of Building Partitions and Elements Using Sound Intensity," American Standard ASTM E 2249 - 02: 2003 (American Society for Testing and Materials 2003).

2. D. Pilon, R. Panneton, and F. Sgard, "Behavioral criterion quantifying the edge-constrained effects on foams in the standing wave tube," J. Acoust. Soc. Am. **114**, 1980–1987 (2003).
3. B. H. Song, J. S. Bolton, and Y. J. Kang, "Effect of circumferential edge constraint on the acoustical properties of glass fiber materials," J. Acoust. Soc. Am. **110**, 2902–2916 (2001).
4. B. H. Song and J. S. Bolton, "Investigation of the vibrational modes of edge-constrained fibrous samples placed in a standing wave tube," J. Acoust. Soc. Am. **113**(4), 1833–1849 (2003).
5. H.S. Tsay and F.H. Yeh, "The influence of circumferential edge constraint on the acoustical properties of open-cell polyurethane foam samples," J. Acoust. Soc. Am. **19**, 2804–2814 (2006).
6. D. Pilon, R. Panneton, and F. Sgard, "Behavioral criterion quantifying the effects of circumferential air gaps on porous materials in the standing wave tube," J. Acoust. Soc. Am. **116**, 334–356 (2004).
7. O. Doutres and N. Atalla, "Acoustic contributions of a sound absorbing blanket placed in a double panel structure: Absorption versus transmission," J. Acoust. Soc. Am. **128**(2), (2010).

8. Anonymous, "Acoustics - Determination of sound absorption coefficient and impedance in impedance tubes. Part 2: Transfer-function method," International Standard ISO-10534-2 (1998).
9. Y. Salissou, "Caractérisation des propriétés acoustiques des matériaux poreux à cellules ouvertes et à matrice rigide ou souple", Ph. D. dissertation. University of Sherbrooke, Québec, (2009).
10. B.H. Song and J.S. Bolton, "A transfer matrix approach for estimating the characteristic impedance and wave numbers of limp and rigid porous materials," J. Acoust. Soc. Am. **107** (3), 1131-1152 (2000).
11. J.F. Allard and N. Atalla, "Propagation of sound in porous media: Modeling sound absorbing materials", Second Edition, Wiley, (2009).
12. R. Panneton, "Comments on the limp frame equivalent model for porous media," J. Acoust. Soc. Am. **122**(6), EL217-222 (2007).
13. O. Doutres, N. Dauchez, J. M. Génevaux, and O. Dazel, "Validity of the limp model for porous materials: A criterion based on the Biot theory", J. Acoust. Am. **122**(4), 2038-2048 (2007).
14. Y. Salissou and R. Panneton, "Pressure/mass method to measure open porosity of porous solids," J. Appl. Phys. **101**, 124913.1-124913.7 (2007).
15. O. Doutres, Y. Salissou, N. Atalla, and R. Panneton, "Evaluation of the acoustic and non-acoustic properties of sound absorbing materials using a three-microphone impedance tube," Appl. Acoust. **71**(6), 506-509 (2010).
16. M.R. Stinson and G.A. Daigle, "Electronic system for the measurement of flow resistance," J. Acoust. Soc. Am. **83**, 2422-2428 (1988).
17. B. Castagnède, A. Aknine, B. Brouard and V. Tarnow, "Effects of compression on the sound absorption of fibrous materials," Appl. Acoust. **61**, 173–182 (2000).
18. C.N. Wang, Y.M. Kuo and S.K Chen, "Effects of compression on the sound absorption of porous materials with an elastic frame," Appl. Acoust. **69**, 31–39 (2008).

19. L. Jaouen and F.X. Bécot, “Reinforcement of acoustical material properties using multiple scales,” proceedings of SIA conference, Le Mans, France (2008).
20. E. Gourdon and M. Seppi, “On the use of porous inclusions to improve the acoustical response of porous materials: Analytical model and experimental verification,” Appl. Acoust. **71**, 283–298 (2010).
21. F.C. Sgard, X. Olny, N. Atalla and F. Castel, “On the use of perforations to improve the sound absorption of porous materials,” Appl. Acoust. **66**, 625–651 (2005).

Table 1. Impedance tube characteristics for the experimental measurements.

Description	**diameter**	**Frequency range**	**Distance mic1-mic2**	**Distance mic2-sample**
Medium impedance tube	44.5 mm	150-4200 Hz	25 mm	45 mm
Large impedance tube	100 mm	70-1900 Hz	50 mm	100 mm

Table 2: Properties of the material samples.

Material properties	**Material A**	**Material B**	**Material C**
Porosity ϕ	0.98	0.99	0.97
Density ρ (kg/m^3)	8.4	5.5	133
Static airflow resistivity σ (Ns/m^4)	10,850	14,000	95,000
Tortuosity α_∞	1	1	-
Viscous length Λ (μm)	87	70	-
Thermal length Λ'(μm)	163	107	-

Figure Captions

Figure 1**:** Schematic view of the double wall structure [7].

Figure 2: Schematic view of the three impedance tube setups: (a) measurement of r_2, (b) measurement of r_1, (c) measurement of TL_m.

Figure 3: 2.0 inch melamine foam: (a) absorption coefficient related to r_1 with D_2=25 mm (b) absorption coefficient related to r_2 (c) sound transmission loss TL_m.

Figure 4: (a) Normal incidence sound transmission loss of the empty structure or filled in with the material A; (b) sound transmission loss contributions of material A.

Figure 5: Homemade sample holder to compress the fibrous sample.

Figure 6: Effect of frame compression on a 2.0 inch fibre glass material: (a) absorption coefficient related to r_1 with D_2=2 mm (b) absorption coefficient related to r_2 and (c) sound transmission loss TL_m.

Figure 7: Effect of frame compression on a 2.0 inch fibre glass material: Transmission loss contribution of the (a) upstream and (b) downstream cavities.

Figure 8: Effect of frame compression on a 2.0 inch fibre glass material: (a) Transmission loss of the double wall structure, (b) Airborne insertion loss.

Figure 9: Perforated rockwool sample with or without a melamine foam inclusion.

Figure 10: Effect of double porosity: (a) absorption coefficient related to r_1 with D_2=10mm (b) absorption coefficient related to r_2 and (c) sound transmission loss of the sample TL_m.

Figure 11: Effect of double porosity: Transmission loss contribution of the (a) upstream and (b) downstream cavities.

Figure 12: Effect of double porosity: (a) Transmission loss of the double wall structure, (b) Airborne insertion loss.

Figure 01

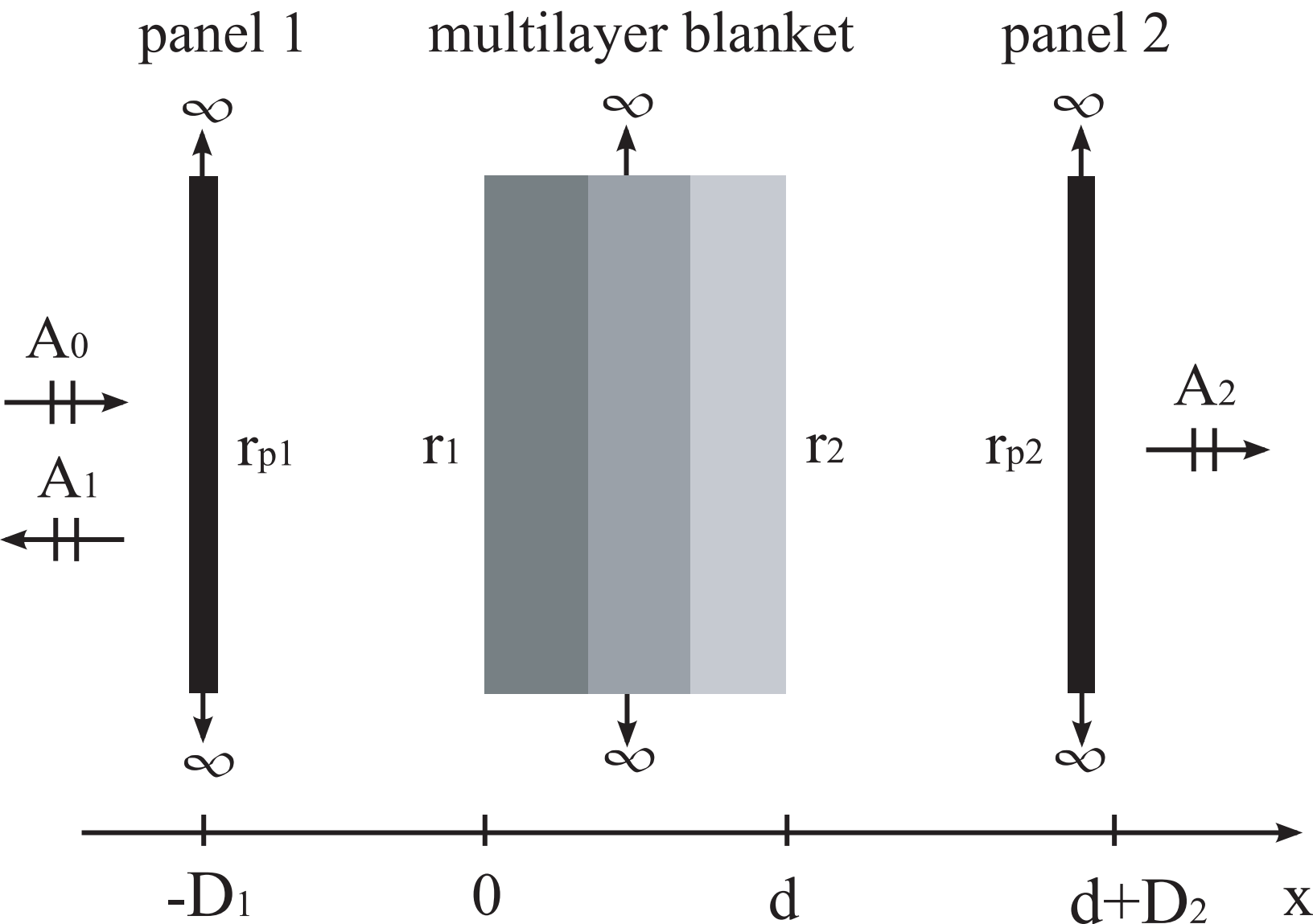
panel 1
multilayer blanket
panel 2
∞
∞
∞
∞
∞
∞
A0
A1
rp1
r1
r2
rp2
A2
-D1
0
d
d+D2
x

Figure 02

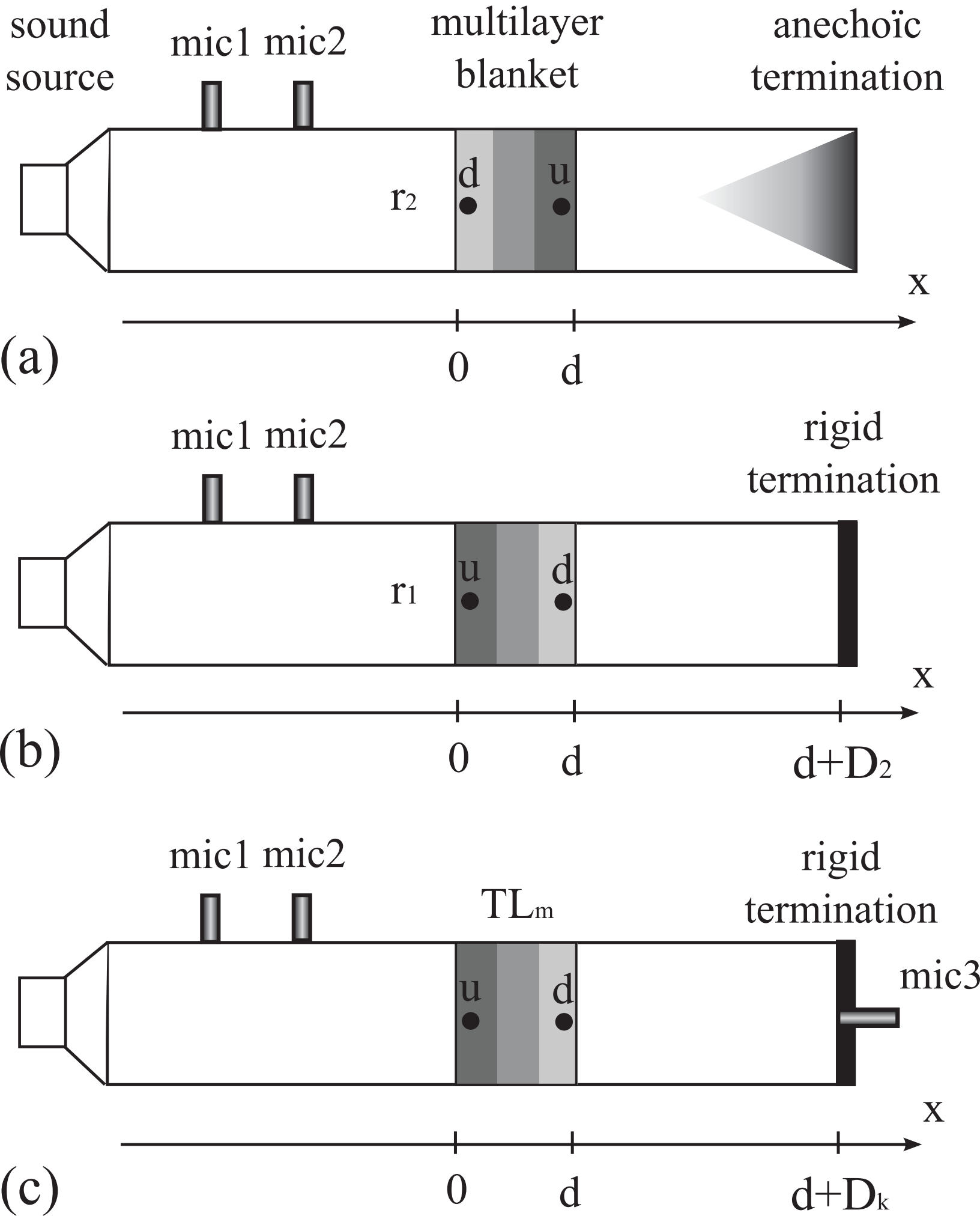
sound source
mic1 mic2
multilayer blanket
anechoïc termination
r2
d
u
x
(a)
0
d
mic1 mic2
rigid termination
r1
u
d
x
(b)
0
d
d+D2
mic1 mic2
TLm
rigid termination
u
d
mic3
x
(c)
0
d
d+Dk

Figure 03

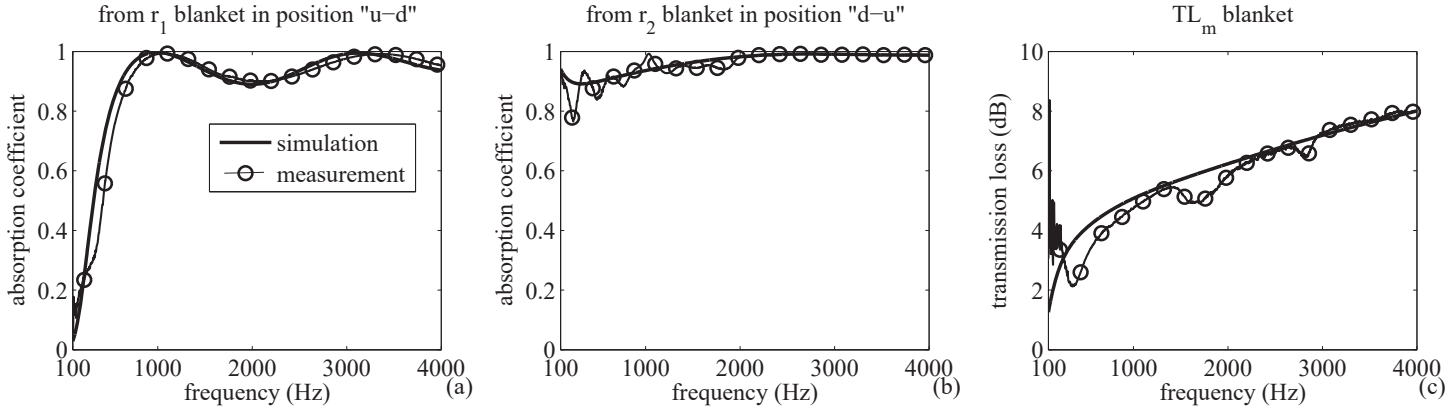
from r1 blanket in position "u−d"
absorption coefficient
frequency (Hz)
simulation
measurement
(a)
from r2 blanket in position "d−u"
absorption coefficient
frequency (Hz)
(b)
TLm blanket
transmission loss (dB)
frequency (Hz)
(c)

Figure 04

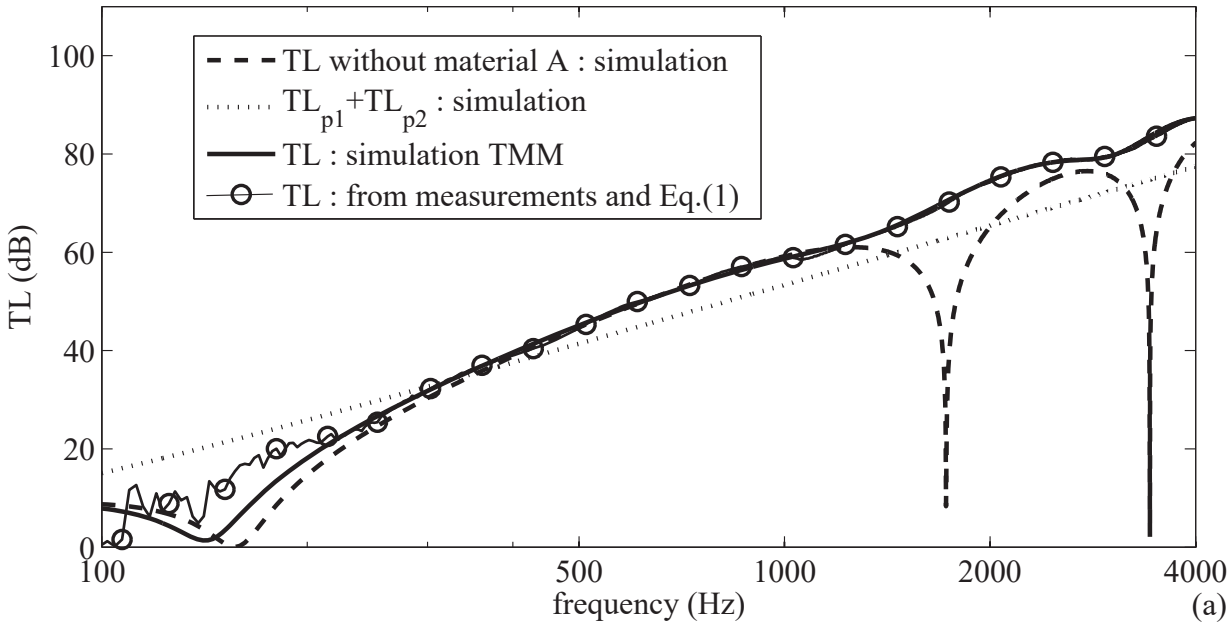
TL without material A : simulation
TL_p1+TL_p2 : simulation
TL : simulation TMM
TL : from measurements and Eq.(1)
TL (dB)
frequency (Hz)
100
500
1000
2000
4000
0
20
40
60
80
100
(a)

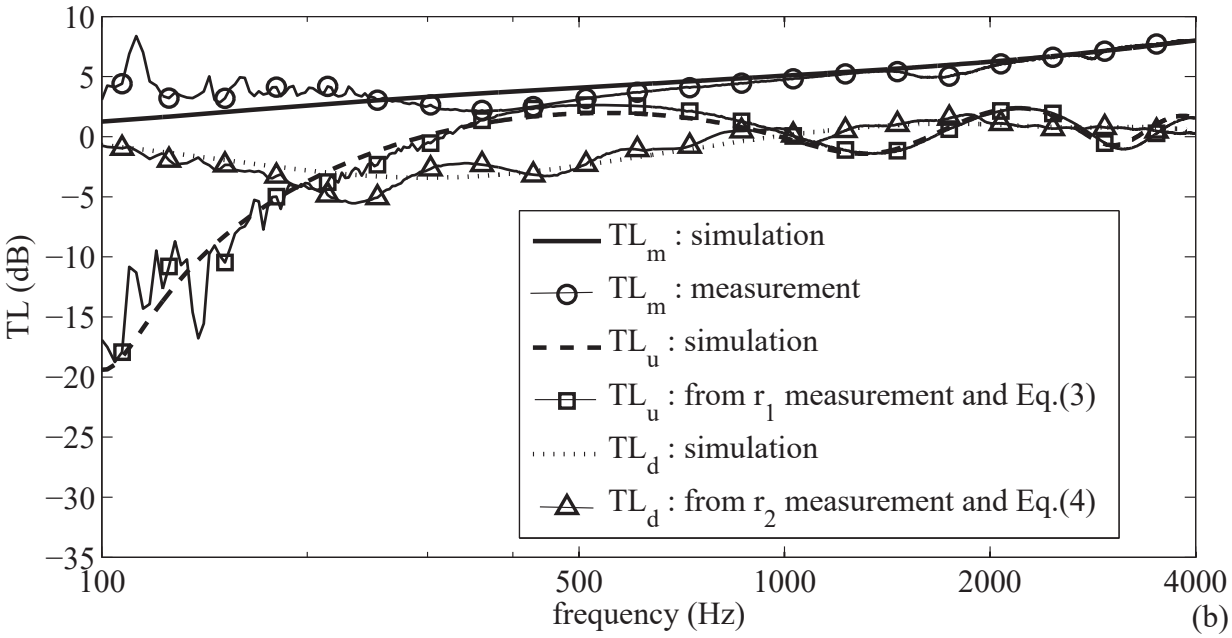
TL_m : simulation
TL_m : measurement
TL_u : simulation
TL_u : from r_1 measurement and Eq.(3)
TL_d : simulation
TL_d : from r_2 measurement and Eq.(4)
TL (dB)
frequency (Hz)
100
500
1000
2000
4000
10
5
0
−5
−10
−15
−20
−25
−30
−35
(b)

Figure 05

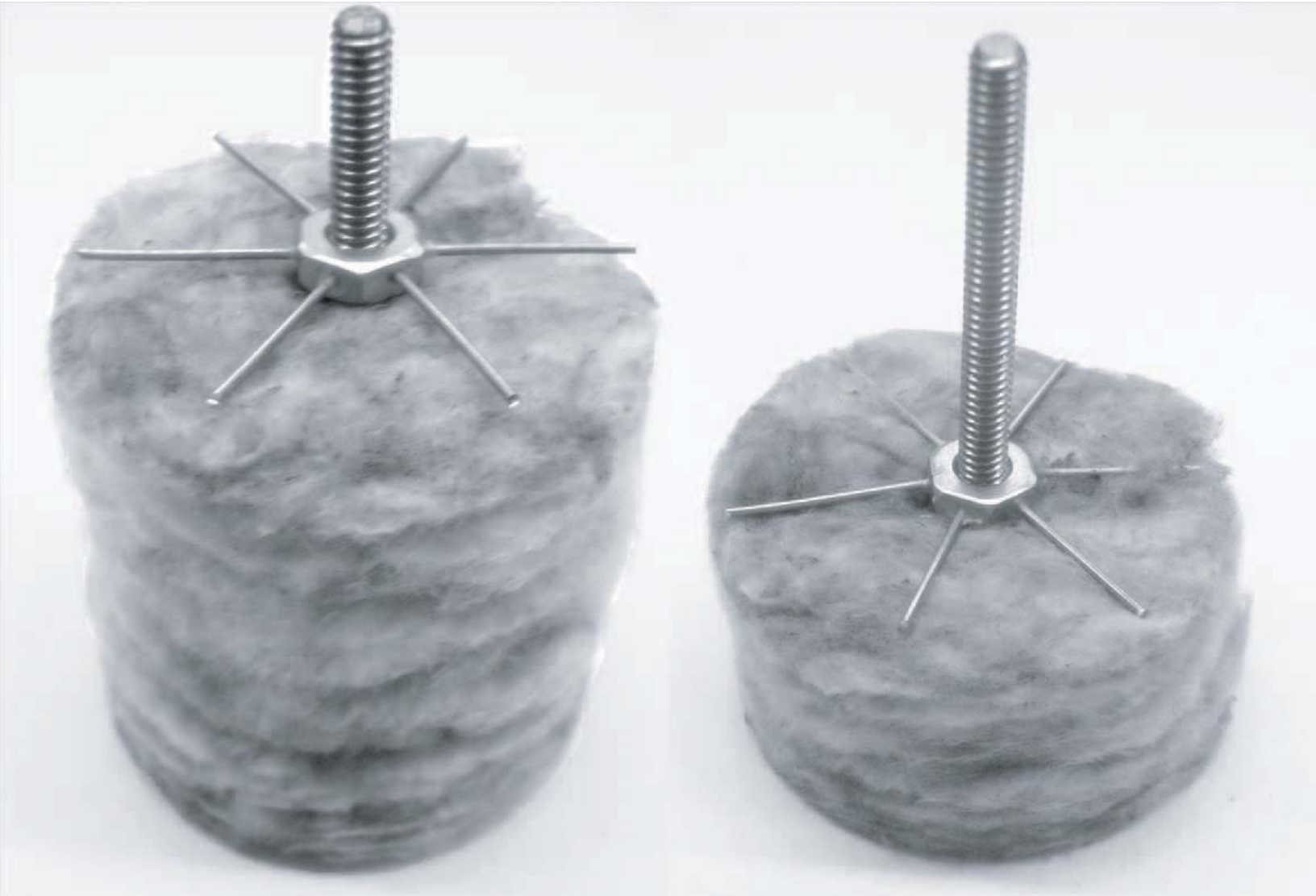

Figure 06

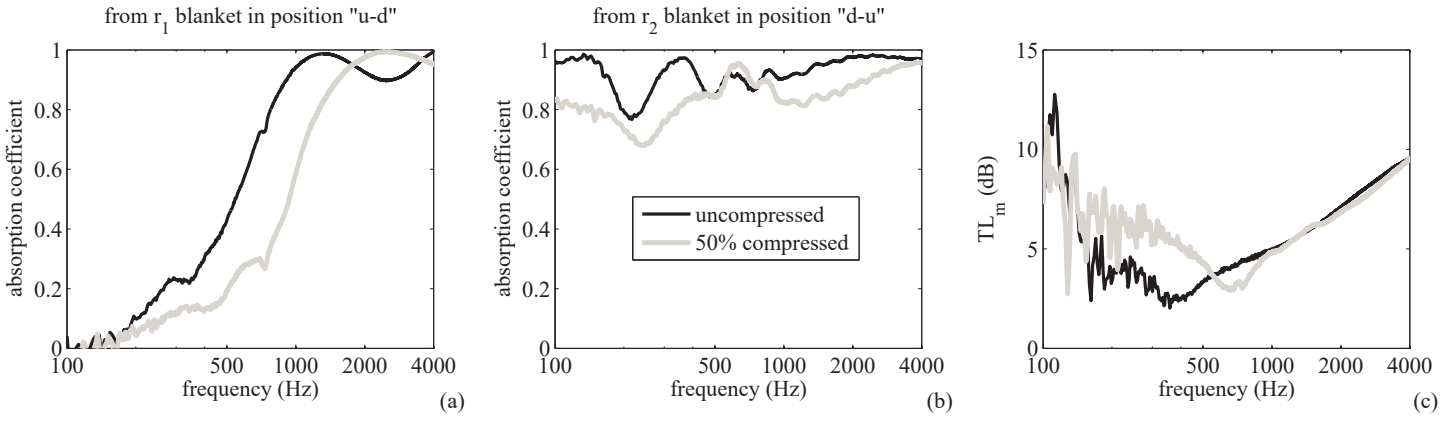
from r1 blanket in position "u-d"
absorption coefficient
frequency (Hz)
(a)
from r2 blanket in position "d-u"
absorption coefficient
uncompressed
50% compressed
frequency (Hz)
(b)
TLm (dB)
frequency (Hz)
(c)

Figure 07

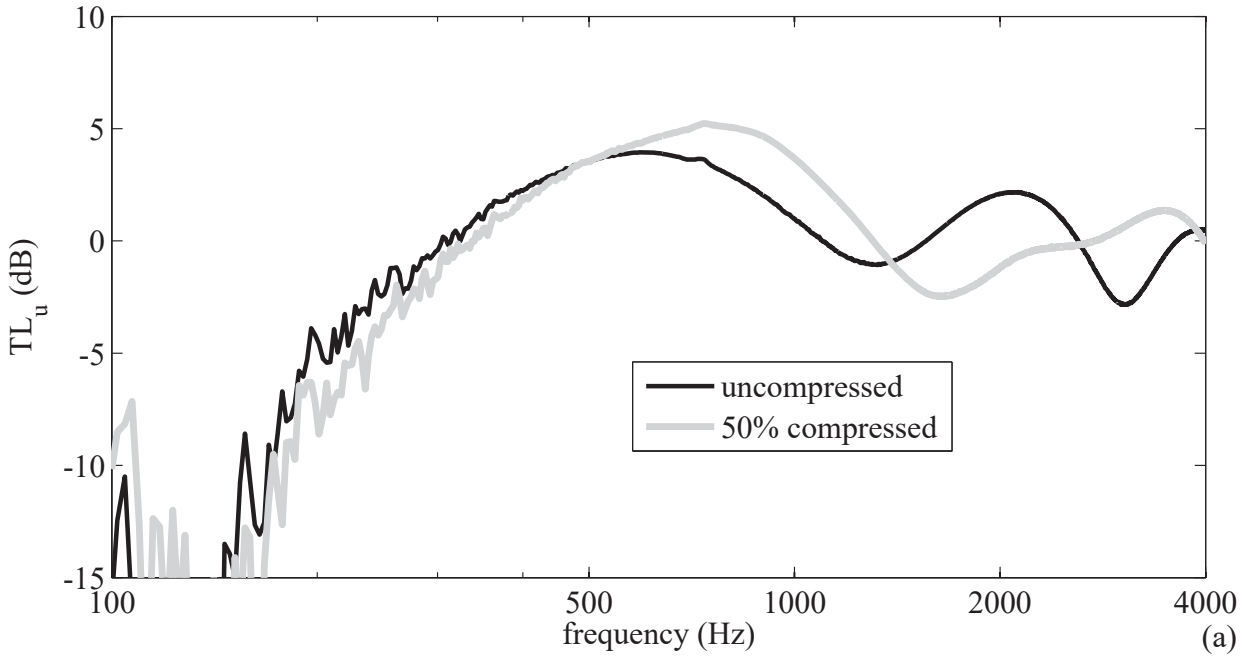
10
5
0
-5
-10
-15
TL_u (dB)
uncompressed
50% compressed
100
500
1000
2000
4000
frequency (Hz)
(a)

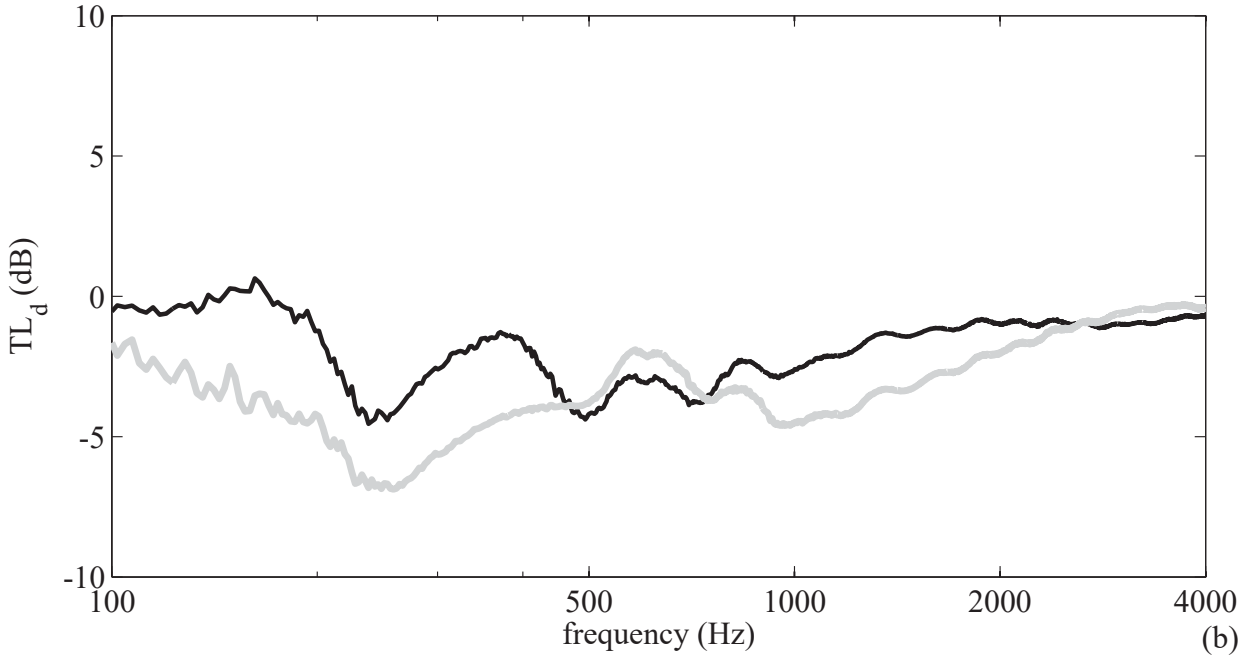
10
5
0
-5
-10
TL_d (dB)
100
500
1000
2000
4000
frequency (Hz)
(b)

Figure 08

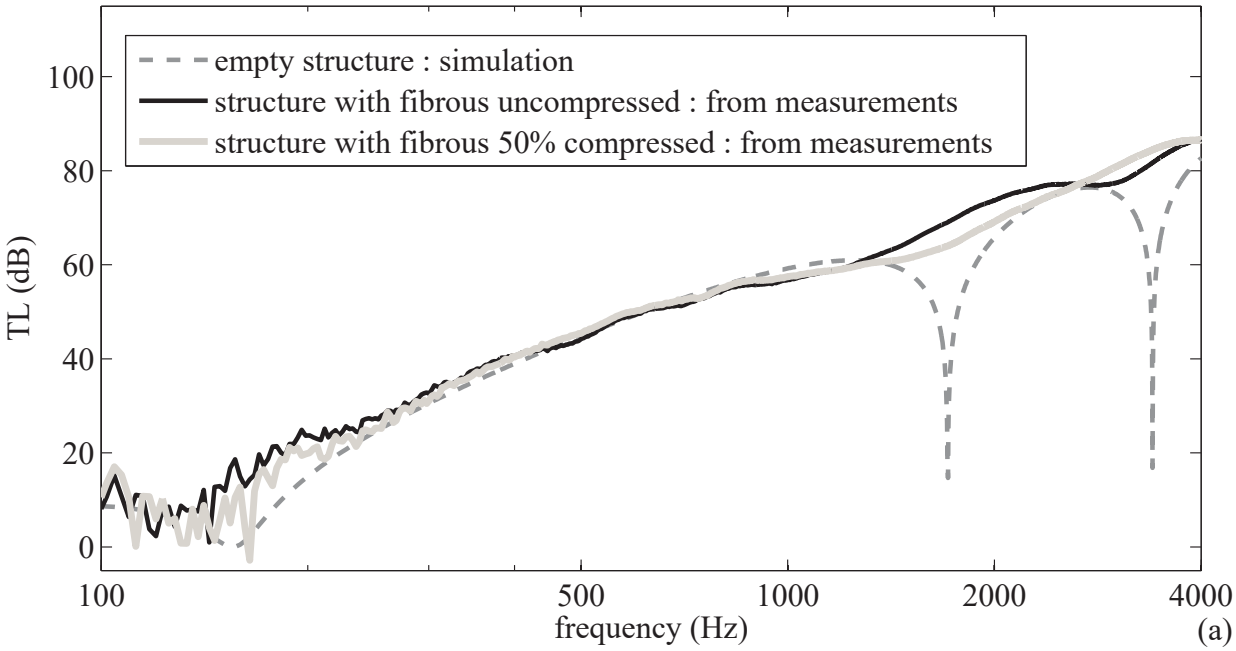
empty structure : simulation
structure with fibrous uncompressed : from measurements
structure with fibrous 50% compressed : from measurements
TL (dB)
100
80
60
40
20
0
100
500
1000
2000
4000
frequency (Hz)
(a)

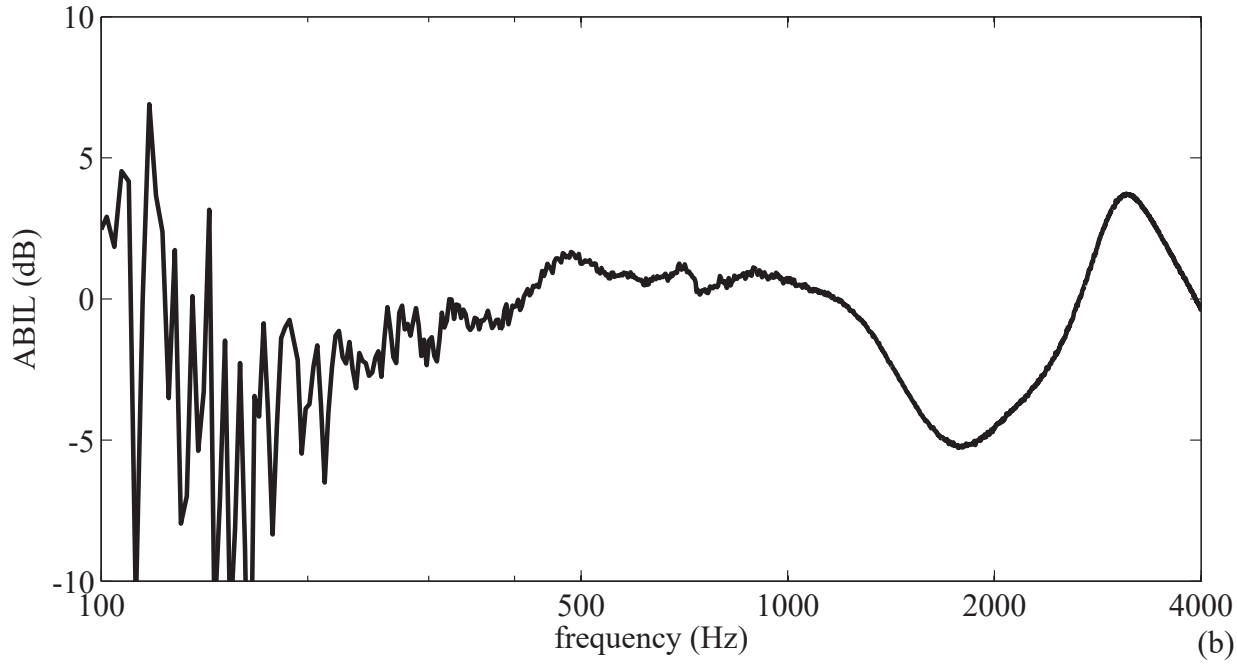
ABIL (dB)
10
5
0
-5
-10
100
500
1000
2000
4000
frequency (Hz)
(b)

Figure 09

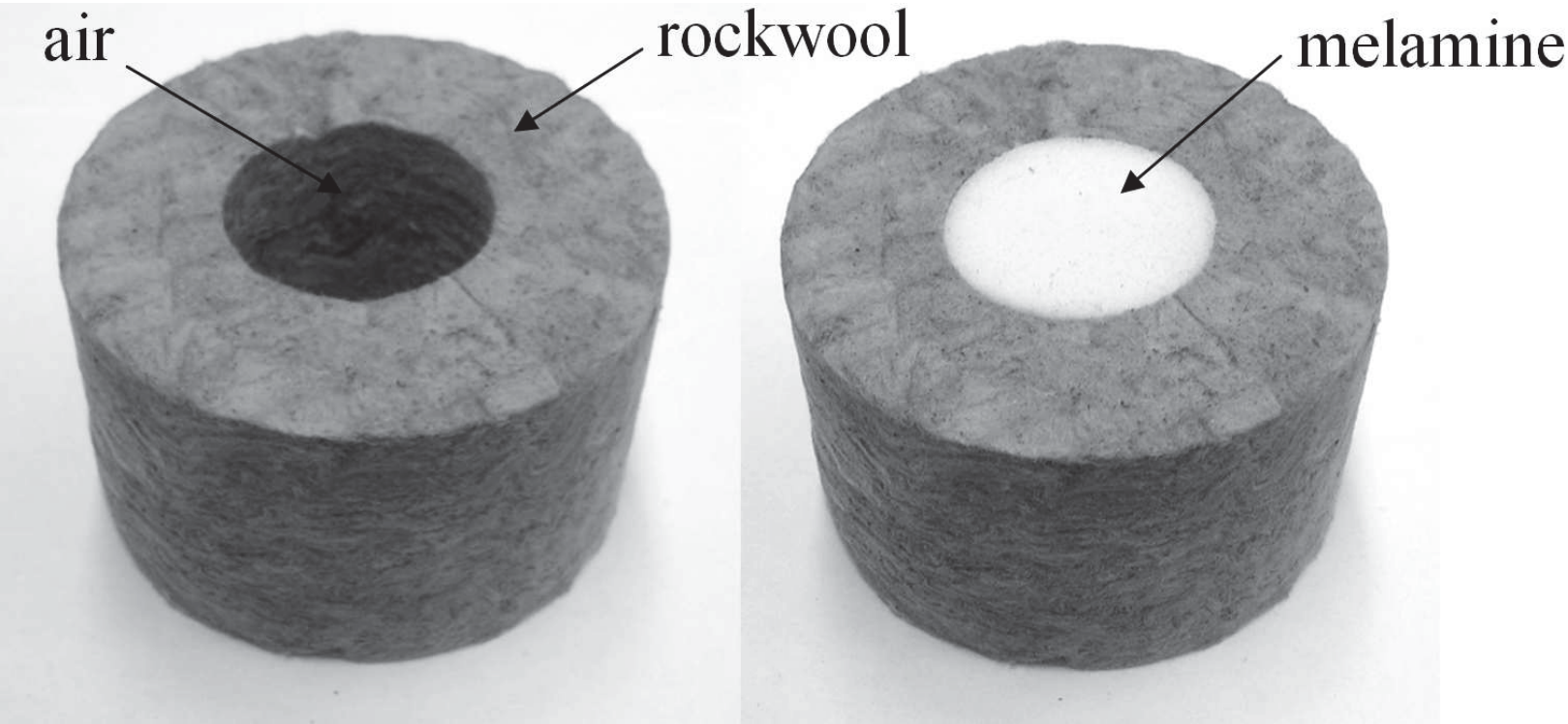

Figure 10

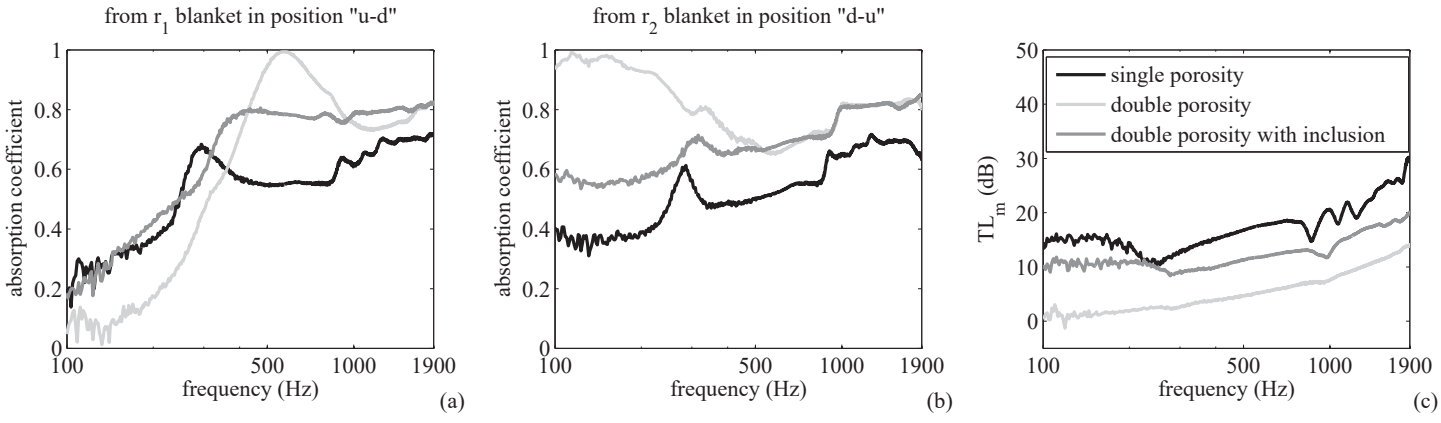
from r1 blanket in position "u-d"
from r2 blanket in position "d-u"
absorption coefficient
frequency (Hz)
TLm (dB)
single porosity
double porosity
double porosity with inclusion
(a)
(b)
(c)

Figure 11

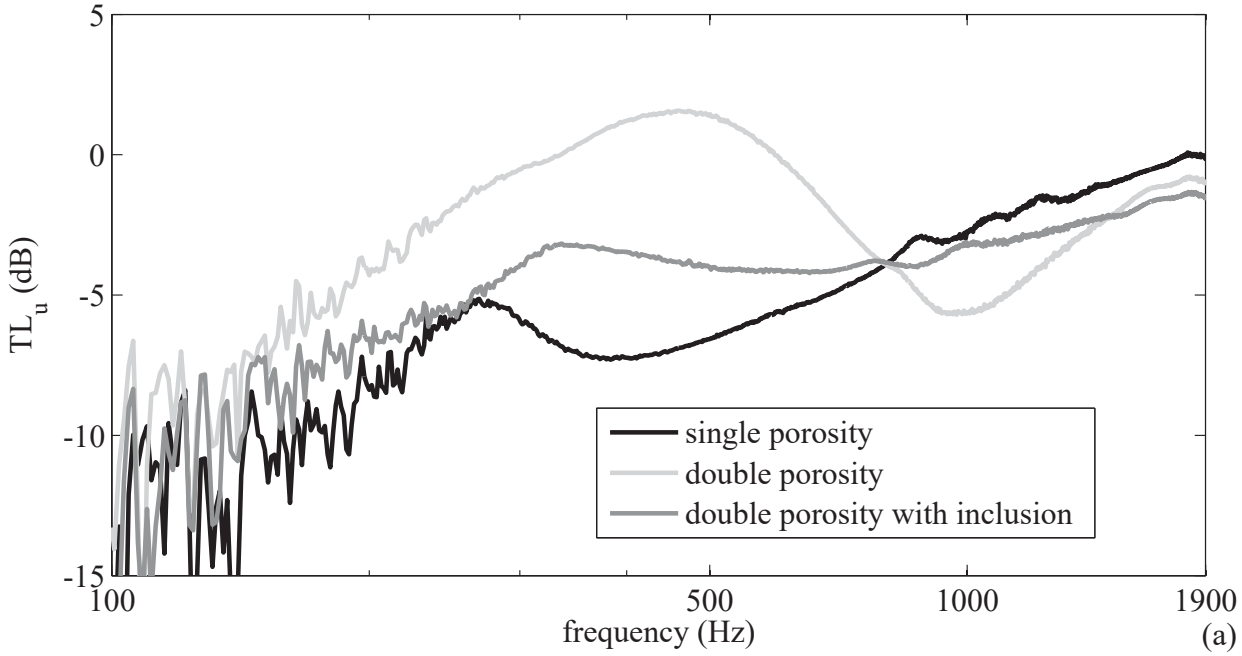
5
0
-5
-10
-15
TL_u (dB)
100
500
1000
1900
frequency (Hz)
single porosity
double porosity
double porosity with inclusion
(a)

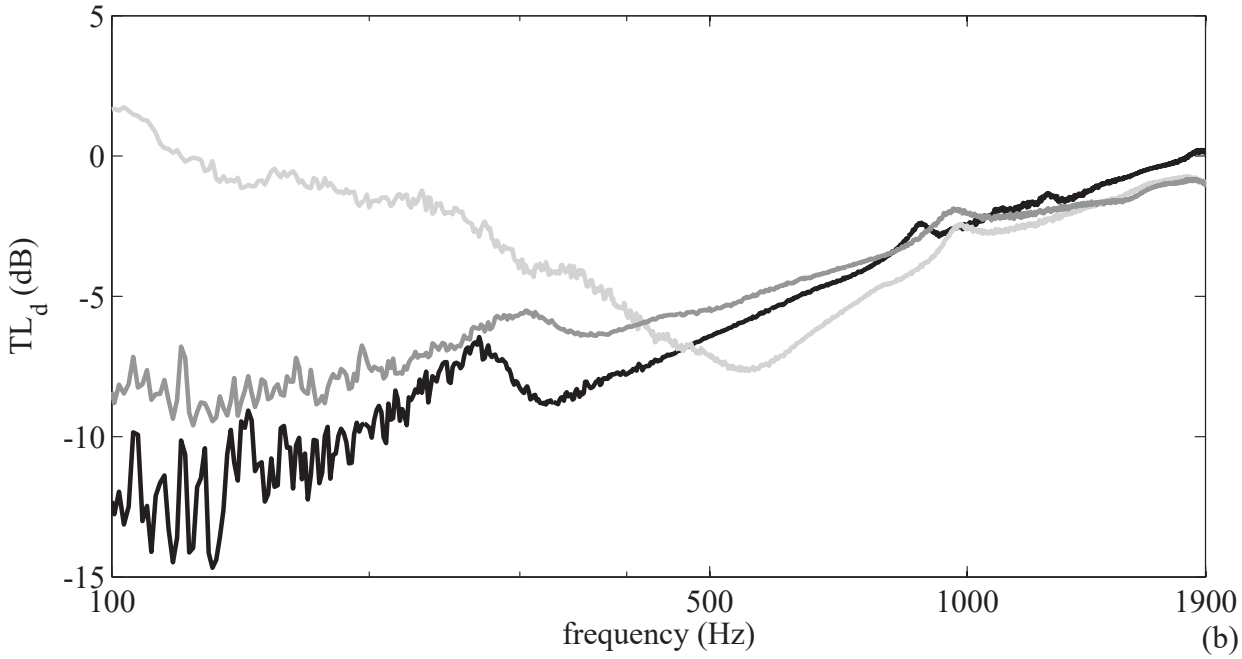
5
0
-5
-10
-15
TL_d (dB)
100
500
1000
1900
frequency (Hz)
(b)

Figure 12

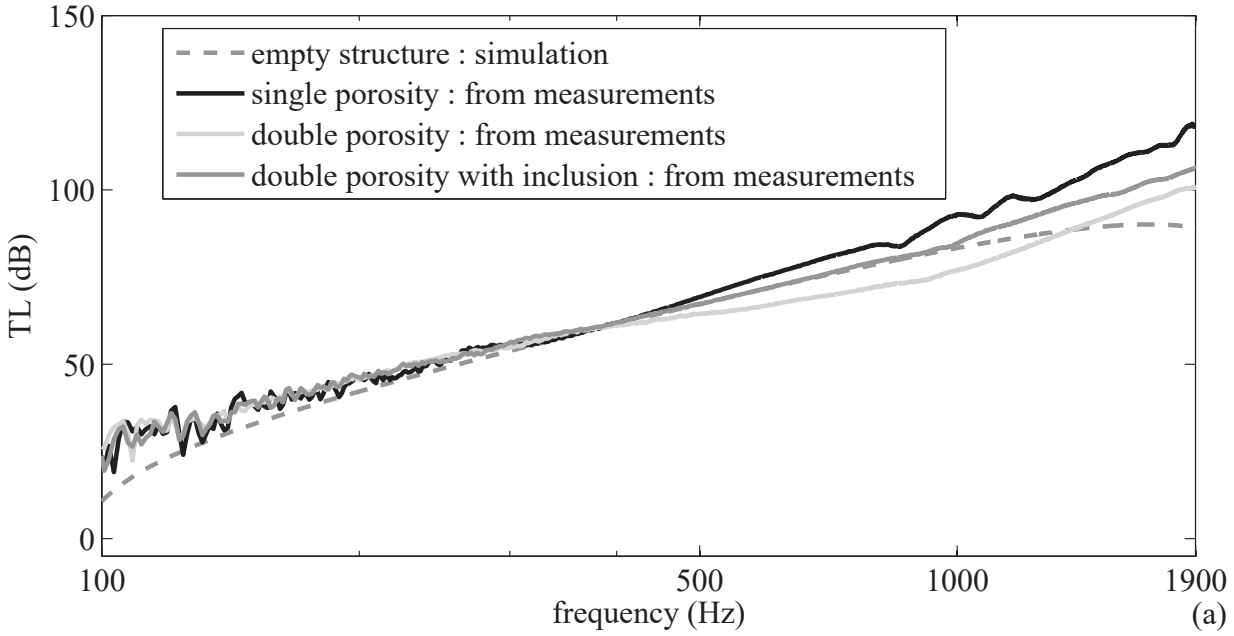
150
100
50
0
TL (dB)
empty structure : simulation
single porosity : from measurements
double porosity : from measurements
double porosity with inclusion : from measurements
100
500
1000
1900
frequency (Hz)
(a)

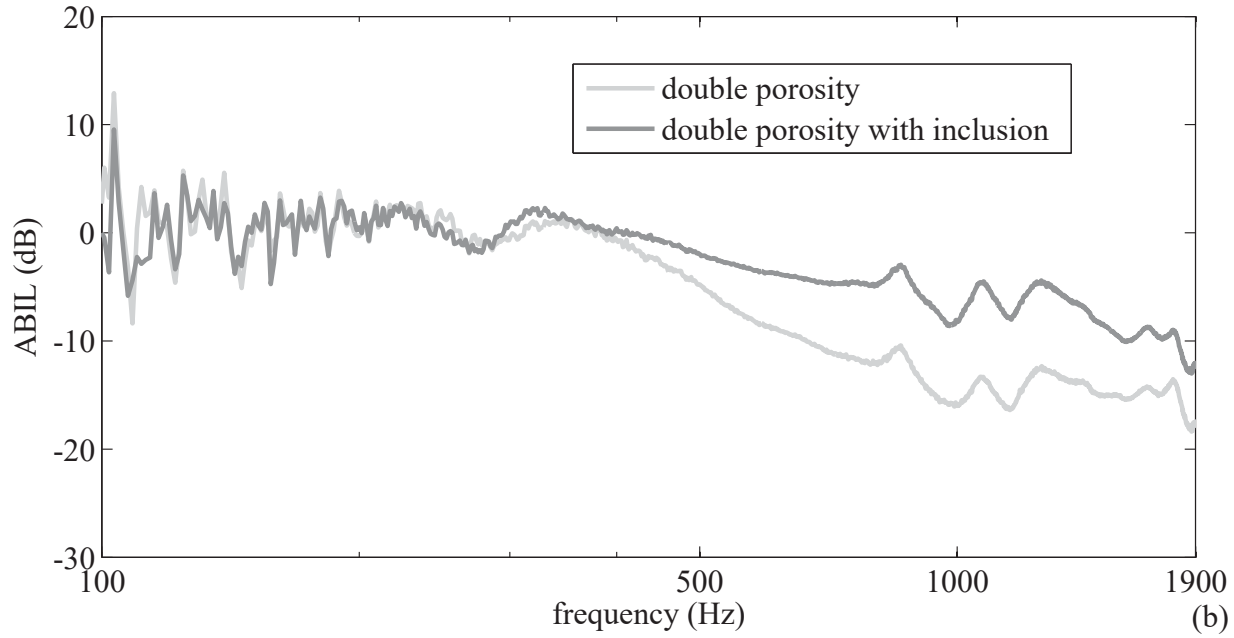
20
10
0
-10
-20
-30
ABIL (dB)
double porosity
double porosity with inclusion
100
500
1000
1900
frequency (Hz)
(b)